



# A GIS method for reconstruction of late Quaternary landscapes from isobase data and modern topography

David W. Leverington\*, James T. Teller, Jason D. Mann

*Department of Geological Sciences, University of Manitoba, Winnipeg, Manitoba, Canada R3T 2N2*

Received 2 January 2001; received in revised form 4 August 2001; accepted 6 August 2001

## Abstract

Digital reconstructions of late Quaternary landscapes can be produced using a geographic information system (GIS) method that subtracts interpolated isobase values from modern elevations and bathymetry. The principal utility of the GIS method for reconstructing late Quaternary landscapes is in the relative ease and rapidity with which high-resolution, quantitative, and georeferenced databases of paleo-topography can be generated. These databases can be used for many purposes, including the generation of paleo-topographic maps, the estimation of the areas and volumes of individual water bodies and landforms, and the approximation of paleo-shoreline positions. GIS-based estimates of the dimensions of water bodies and landforms can be used to help constrain hydrological and climatic models of the late Quaternary. © 2002 Elsevier Science Ltd. All rights reserved.

*Keywords:* Geographic information system (GIS); Paleo-topographic model; Isostatic rebound; Late Quaternary

## 1. Introduction

The general form of a glacial or post-glacial landscape can be reconstructed for a particular time interval by subtracting interpolated isobase values from modern elevations. Paleo-topographic information is useful for the characterization of past environments, and for the assessment and modelling of past geological, hydrological, and climatic processes (e.g., Mann et al., 1997; Gareau et al., 1998; Leverington et al., 2000). Although generalized reconstructions of late Quaternary landforms can be produced from isobase data and modern topography using manual methods, the time-consuming and tedious nature of this approach is not suitable for the rapid generation of large, high-resolution databases of paleo-topography.

This paper presents an overview of the methodologies and issues involved in the use of GIS techniques for

modelling the topography (elevations and bathymetry) of late Quaternary landscapes from isobase data and modern topography. A database of paleo-topography for the central Canadian Arctic at 9300  $^{14}\text{C}$ yr BP is generated in order to demonstrate the method.

## 2. Glacio-isostatic rebound and isobase maps

During glaciation, the formation and expansion of an ice sheet loads the Earth's crust, causing terrain subsidence below the ice sheet and in broad regions adjacent to its margins (Walcott, 1970; Peltier, 1974, 1985; Peltier and Andrews, 1976). The reduction of ice mass causes terrain emergence during and following deglaciation through the process of glacio-isostatic rebound (e.g., Walcott, 1972; Farrell and Clark, 1976; Clark et al., 1978; Andrews, 1989). The extent to which the surface of a region has been uplifted since a given time can be estimated if segments of strandlines, formed at the time of interest and associated with an extensive body of water, are widely distributed in the region. The regional pattern of emergence can be approximated by

\*Corresponding author. Center for Earth and Planetary Studies, National Air and Space Museum, Smithsonian Institution, Washington, D.C., 20560-0315.

*E-mail address:* leveringtond@nasm.si.edu (D.W. Leverington).

plotting the modern elevations of the once-horizontal but now differentially raised strandlines of a particular age on a map.

If sufficient strandline evidence is available, the configuration of the former marine or lacustrine surface can be approximated, either manually or by quantitative methods such as trend surface analysis, with lines of equal isostatic rebound (*isobases*) used to describe the relative uplift of any former surface (e.g., Johnston, 1946; Andrews, 1966, 1970; McCann and Chorley, 1967; Smith et al., 1969; Blake, 1970; Andrews et al., 1971; Dyke, 1974). Isobases are contours that can be used to portray the relative morphometry of time-equivalent crustal deformation resulting from glacial unloading (Andrews, 1970), although isobases can additionally be a function of hydro-isostatic effects (e.g., Farrell and Clark, 1976; Clark et al., 1978), ice-sheet gravitational effects (e.g., Clark, 1976), and changes in sea level (e.g., Andrews, 1970, 1989; Walcott, 1972).

### 3. GIS reconstruction of late Quaternary landscapes

#### 3.1. Methodology

Late Quaternary landscapes of isostatically deformed regions can be reconstructed most easily and accurately by using a geographic information system (GIS), because a GIS can facilitate the collection of relevant topographic and isobase data, can be used to interpolate these values to continuous surfaces, and can be used to perform spatial arithmetic. In addition, quantitative analyses of the resulting paleo-topographic database (e.g., calculations of area, volume, aspect, and slope) can be performed using standard GIS tools, and specialized data products such as topographical cross-sections, histograms of bathymetry, and three-dimensional views or animations can be generated. The raster data format is the most appropriate GIS data structure for use in reconstructing late Quaternary landscapes because it is ideally suited for arithmetic using multiple spatial datasets.

The use of a GIS in the raster-based reconstruction of a glacio-isostatically deformed late Quaternary landscape first involves the generation of a single data layer for each of (1) modern topography, and (2) interpolated isobase values (or, alternatively, interpolated shoreline-elevation point data). If these two data layers are georeferenced to each other, have been resampled to a common grid resolution, and contain values expressed with respect to a common datum, then a database of paleo-topography, in which elevations and bathymetry are given with respect to the restored water plane, can be generated by subtracting the interpolated isobase values from modern elevations. This calculation adjusts topography for the effects of isostatic rebound since the time

period being modelled, and also adjusts for other effects such as changes in sea level (Fig. 1). Paleo-topographic databases, generated through the adjustment of modern elevations using raised-shoreline data, can be used in the quantitative characterization of terrain morphology and surface processes (e.g., Lambeck, 1996; Mann et al., 1997, 1999; Gareau et al., 1998; Leverington et al., 2000).

There are several limits associated with the GIS method: (1) the method can only be applied to regions where the amounts of deposition and erosion of earth materials since the time being modelled are small compared to the landscape as a whole (Lambeck, 1996; Mann et al., 1999); (2) poor results will be produced if modelling involves oversimplification of the nature of relative isostatic rebound; and (3) databases must have horizontal and vertical resolutions fine

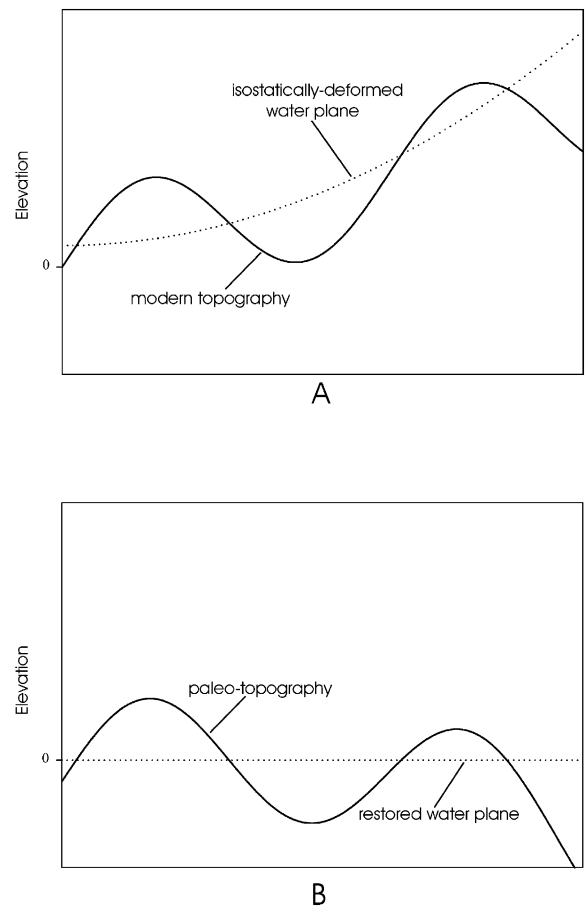


Fig. 1. A: Schematic cross-section of modern topography and deformed water plane (i.e., an isobase surface); elevations in A are specified relative to modern sea level. B: Schematic cross-section of paleo-topography and restored (flattened) water plane; elevations in B are specified relative to restored water plane.

enough to satisfy the modelling and reconstruction goals, or else results will be of limited value and potentially deceptive and inaccurate.

### 3.2. Constructing a database of modern elevations

Global databases of modern topography are now widely available in raster format at little or no cost, and have been assembled from a variety of public-domain data sources. Notable global databases include the GLOBE database (land data;  $30 \times 30$  arcsec cells (GLOBE Task Team, 1999)), the GTOPO 30 database (land data;  $30 \times 30$  arcsec cells (EDC DAAC, 1996)) and the ETOPO 5 database (land and ocean data;  $5 \times 5$  arc-min cells (NGDC, 1988)). These global databases are especially useful when modelling regions that are hundreds or thousands of kilometres in dimension, as the resolution of these databases is sufficiently fine to generate useful landscape reconstructions for these regions, yet is sufficiently coarse to keep database sizes manageable. These databases often cannot be used for the modelling of smaller regions (e.g., tens to hundreds of kilometres in dimension) because, at larger scales, their relatively low spatial resolutions may not properly define otherwise distinct and significant topographic features. Furthermore, database artifacts, such as the abrupt topographic discontinuities that are sometimes present at the boundaries between individual sub-databases, can become increasingly discernable and problematic at larger scales (these discontinuities are typically caused by factors such as differing data qualities, resolutions, or resampling schemes). Smaller regions should be modelled using higher-resolution raster elevation data. Although the geographic availability of digital topographic data with horizontal resolutions of less than about 50 m is currently somewhat restricted (especially for large, sparsely populated regions), the ongoing generation of regional high-resolution topographic models from, for example, space-based radar measurements (JPL, 1998), will make these data more widely available in the future.

Regardless of the data source used, topographic databases should not be employed for the reconstruction of Quaternary landscapes without an assessment of database quality and applicability within the region of interest. In some cases, topographic databases will not be suitable for use because of limitations related to spatial resolution or database accuracy. While the global databases discussed above are generally of sufficient quality for regional paleo-topographic reconstructions, vertical deviations between database and actual elevations can, in the most rare and extreme cases, be as great as hundreds of metres (e.g., Hastings and Dunbar, 1998).

### 3.3. Constructing a database of interpolated isobase values

Once entered into a GIS by keyboard or by hand-digitization from existing maps, isobase data (or, alternatively, shoreline-elevation point data) must be interpolated to a continuous surface and then resampled to the grid resolution of the database of modern elevations. The interpolation of isobase lines produces a continuous *isobase surface* (also termed a *rebound surface* by Mann et al., 1999; Leverington et al., 2000), which can be used to describe the relative glacio-isostatic rebound that has occurred over a region since a given point in time. Within the geographical limits of the water body whose shorelines were used to generate the isobase map, the geometry of an isobase surface will correspond to the geometry of the corresponding (and now isostatically deformed) water plane.

The *triangulated irregular network* (TIN) algorithm (Peucker et al., 1978) has been generally found to produce good results when generating an isobase surface from point or curve data (Mann et al., 1999; Leverington et al., 2000). The TIN data format, which uses straight-edged triangular facets to define a surface, can produce suitable isobase surfaces from relatively complex isobase curves, and is especially useful in the interpolation of gently curving or straight isobases from point data. By comparison, linear and non-linear inverse-distance interpolators have been found to produce isobase surfaces that typically contain unacceptable interpolation irregularities such as localized pits and mounds.

Advanced geostatistical interpolation techniques such as kriging (e.g., Burrough and McDonnell, 1998) in some cases will be preferable alternatives to the TIN algorithm, especially when producing interpolations from relatively sparse isobase datasets. Geostatistical methods of interpolation can be very effective in producing smooth isobase surfaces from widely spaced isobase or beach data, while the fit of the TIN model in such cases can be greatly limited by the planar geometry of component triangular facets.

The above empirical methods of isobase-surface generation can be supplemented or replaced by geophysical methods for modelling crustal dynamics. Such methods can be especially valuable when estimates of rebound magnitude must be made for large regions of land or water where raised-beach data are unavailable (e.g., Lambeck, 1996; Lewis and Gareau, 2001).

The utility of an empirically generated isobase surface in the reconstruction of a late Quaternary landscape is largely a function of: (1) the accuracy of original shoreline elevation and age measurements; (2) the number and geographic distribution of original shoreline measurements; and (3) the general validity of the interpolation methods used to generate isobase lines and the isobase surface itself. Common sources of error

regarding the measurement of elevations and ages of shorelines are summarized by Andrews (1970, 1989).

#### 4. Reconstruction of the landscape of the central Canadian Arctic at 9300 $^{14}\text{C}$ yr BP

##### 4.1. Introduction

A demonstration of the generation of a database of paleo-topography using the GIS method described above is given here for the central Canadian Arctic (Fig. 2) at 9300  $^{14}\text{C}$  yr BP. At its maximum during the late Wisconsinan, the Laurentide Ice Sheet extended from the Arctic mainland of Canada across Victoria, Prince of Wales, and Somerset islands to the southernmost extents of Melville and Bathurst islands (Bryson et al., 1969; Dyke et al., 1982; Dyke, 1984, 1987; Hodgson et al., 1984; Dyke and Prest, 1987). The maximum extent of glacial ice in the Queen Elizabeth Islands during the late Wisconsinan remains uncertain (e.g., Mayewski et al., 1981; Dyke, 1984, 1999; England, 1998; England, 1999; Wolfe and King, 1999).

A small-scale summary of paleo-elevation and ice extent for northern North America at 9000  $^{14}\text{C}$  yr BP is given by Dyke and Prest (1987), and an updated summary of ice extent in the Canadian Arctic for this period is provided by Dyke et al. (1996a). At this time, the ice of the M'Clintock Dome, the northwestern part

of the Late Wisconsinan Laurentide Ice Sheet, extended northward from the mainland to southeastern Victoria Island and southwestern Boothia Peninsula, and completely covered King William Island (Fig. 2). Ice of the Foxe Dome covered much of Melville Peninsula and Baffin Island. Ice coverage elsewhere in the region at 9000  $^{14}\text{C}$  yr BP was generally limited to Cornwallis, Devon, Axel Heiberg, and Ellesmere islands (Dyke and Prest, 1987; Dyke et al., 1996a). The channels of the central Canadian Arctic were mostly free of glacial ice at this time, and significant portions of islands that are now subaerially exposed were flooded by channel waters (e.g., Dyke and Prest, 1987; Dyke et al., 1991, 1996a). Shoreline elevation points for 9300  $^{14}\text{C}$  yr BP are widely distributed in the central Canadian Arctic, and have been used for the construction of regional isobase maps for this time (Dyke, 1984; Dyke et al., 1991).

##### 4.2. Reconstruction of paleo-topography

In order to reconstruct the paleo-topography of the central Canadian Arctic at 9300  $^{14}\text{C}$  yr BP using the GIS method, an isobase surface (i.e., a database of interpolated isobase values - see Section 3.3 above) and a database of modern topography were assembled for the region. Modern land elevations for the database of modern topography (Fig. 3) were extracted from the GLOBE database (cells in this database have a latitude-longitude grid spacing of 30 arc seconds (GLOBE Task Team, 1999)). Modern bathymetric data were extracted from the ETOPO 5 database (cells in this database have

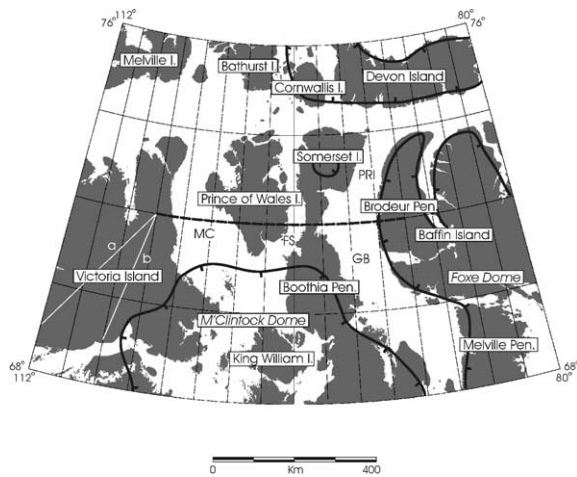


Fig. 2. Map of central Canadian Arctic. Approximate extent of glacial ice at 9000  $^{14}\text{C}$  yr BP is given by thick black lines (after Dyke and Prest, 1987; Dyke et al., 1996a). Locations of two Victoria Island topographic cross-sections (see Fig. 6) are given by white lines, and location of cross-section along 72°N (see Fig. 7) is given by dashed black line. Selected channels are labelled as follows: MC, M'Clintock Channel; FS, Franklin Strait; PRI, Prince Regent Inlet; and GB, Gulf of Boothia. Grid cells are 2° by 2°.

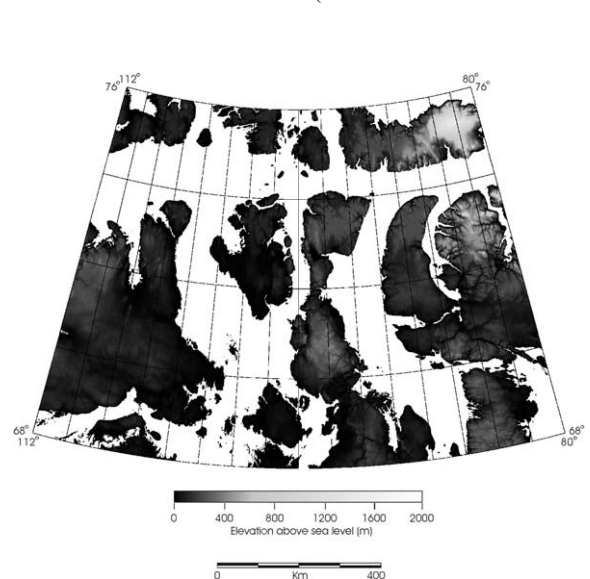


Fig. 3. Map of modern topography for central Canadian Arctic [land data derived from GLOBE 1.0 database (GLOBE Task Team, 1999)]; for clarity, bathymetric data [also used in this study, and extracted from ETOPO 5 database (NGDC, 1988)] are not shown.

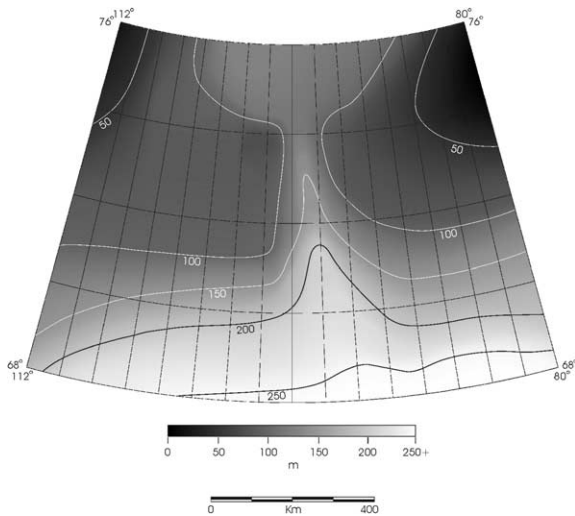


Fig. 4. Map of isobase surface for central Canadian Arctic for 9300  $^{14}\text{Cyr BP}$ , interpolated from compilation of isobase data of Dyke et al. (1991). Isobases (i.e., contours on isobase surface) are given, with values expressed in metres.

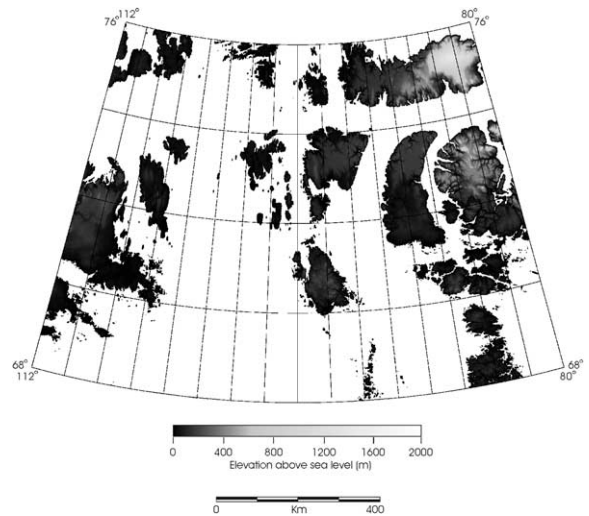


Fig. 5. Map of paleo-topography for central Canadian Arctic at 9300  $^{14}\text{Cyr BP}$ , generated by subtracting isobase surface (Fig. 4) from database of modern topography (Fig. 3). For clarity, bathymetric data are not shown.

a latitude-longitude grid spacing of 5 arc minutes (NGDC, 1988)).

The isobase surface (Fig. 4) was generated from the regional isobase map of Dyke et al. (1991) using the following steps: 1) all isobases were manually entered into a GIS by hand-digitization, generating a set of vectors encoded with rebound values; isobase data for small parts of the Dyke et al. (1991) isobase map that did not contain data, such as the mainland region south of Victoria Island and Boothia Peninsula and the Melville Peninsula region, were extrapolated using the trends of the isobase maps of Dyke (1984) and Andrews (1989); 2) isobase values for locations between isobase vectors were interpolated using the TIN algorithm (see Section 3.3 above) to produce a 3-dimensional model of the isobase surface; 3) the TIN model was converted to raster format, with cells resampled to the spatial resolution of the database of modern elevations; and 4) the raster isobase surface was georeferenced in terms of degrees longitude and latitude.

The isobase surface (Fig. 4), like the isobases from which it was derived, shows that the 9300  $^{14}\text{Cyr BP}$  shoreline rises from low elevations of less than 50 m around Melville Island and eastern Devon Island, to elevations in excess of 250 m south of Boothia Peninsula. The isobase surface is characterized by a pronounced ridge centred on Boothia Peninsula, which does not coincide with the centre of glacial loading in the region (Figs. 2 and 4), as noted by Dyke et al. (1991).

With both the database of modern topography (Fig. 3) and the isobase surface (Fig. 4) having identical geographic extents and cell sizes, a database of paleo-

topography (Fig. 5) was produced by subtracting the isobase surface from the database of modern elevations. This database of paleo-topography delineates the approximate shoreline and subaerial extent of the region's islands at 9300  $^{14}\text{Cyr BP}$ , and is a topographic and bathymetric model of the region at that time. The outline of sea level depicted in Fig. 5 resembles that shown on the map for 9000  $^{14}\text{Cyr BP}$  in Dyke and Prest (1987), and shows that much of the land area now exposed in the region was below sea level at 9300  $^{14}\text{Cyr BP}$ . The total land and channel surface areas in the paleo-topographic model (bounded by latitudes 68° to 76°N and longitudes 80° to 112°W) are 258,188 and 718,772  $\text{km}^2$ , respectively. By comparison, modern land and channel surface areas in this region (Fig. 3) are about 528,643 and 448,317  $\text{km}^2$ , respectively, indicating that land surface area in the region at 9300  $^{14}\text{Cyr BP}$  was about 50% less than today.

The surface areas of different land units in the region were affected in different ways by isostatic and sea-level influences at 9300  $^{14}\text{Cyr BP}$ , depending on their topographic characteristics and the nature of local isostatic depression. For example, the surface area of Brodeur Peninsula (Baffin Island; Fig. 2) was only about 18% less than today (the surface area of the peninsula as described by the paleo-topographic model was 28,173  $\text{km}^2$ , compared with a model surface area of 34,268  $\text{km}^2$  for modern times), due to its relatively steep shorelines and its location in a region where isostatic depression was low relative to land elevations. Similarly, the surface area of Somerset Island was about 18% less than today (20,437  $\text{km}^2$ , compared with 24,786  $\text{km}^2$ ).

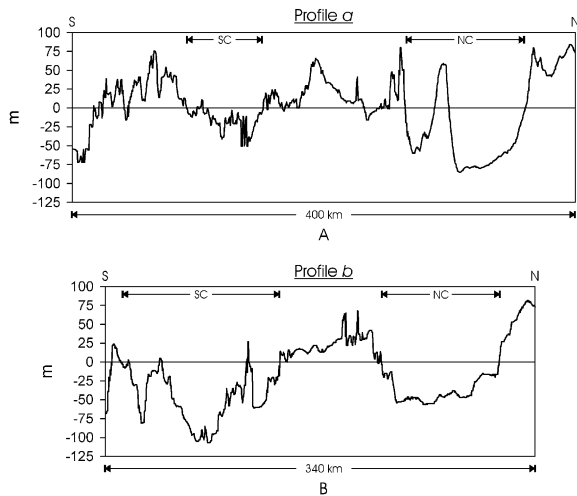


Fig. 6. Topographic cross-sections across two major channels that divided Victoria Island at 9300  $^{14}\text{C}$  yr BP (NC, north channel; SC, south channel). Profile *a* (A) extends from 106°W, 72°N, to 112°W, 69°N; profile *b* (B) extends from 106°W, 72°N to 108°W, 69°N (profile locations are given by white lines in Fig. 2). Elevations are given with respect to sea level at 9300  $^{14}\text{C}$  yr BP. Vertical exaggeration is 600  $\times$ .

Land units with relatively low elevations generally suffered much greater decreases in exposed surface area at 9300  $^{14}\text{C}$  yr BP. For example, the surface area of Prince of Wales Island was about 73% less than today (9418 km<sup>2</sup>, compared with 34,977 km<sup>2</sup>). Low-elevation land units located in regions of considerable isostatic depression (e.g., King William Island) were entirely below sea level at this time.

While the eastern part of Victoria Island was below sea level at 9300  $^{14}\text{C}$  yr BP, the western part was divided by two large channels (Fig. 5; see also, e.g., Dyke and Prest, 1987), each with a length of about 300 km. Paleotopographic cross-sections of these channels, derived from the paleo-topographic model (Fig. 5), are given in Fig. 6. The paleo-topography suggests that the Victoria Island channels were sufficiently large to influence water circulation in the region surrounding Victoria Island (if flow through the channels was not blocked in the southeast by the Laurentide Ice Sheet), with maximum channel depths in any given section typically exceeding 50 m, and channel widths ranging between about 30 and 90 km. The opening and subsequent closing of these large channels may have influenced land- and sea-animal migration in the area, as well as the transport of water-borne arctic wood (see also Dyke et al., 1996a, b, 1997).

While isostatic depression in the arctic islands greatly influenced the distribution of exposed land at 9300  $^{14}\text{C}$  yr BP, its associated influence on the morphology and size of major channels in the region was equally

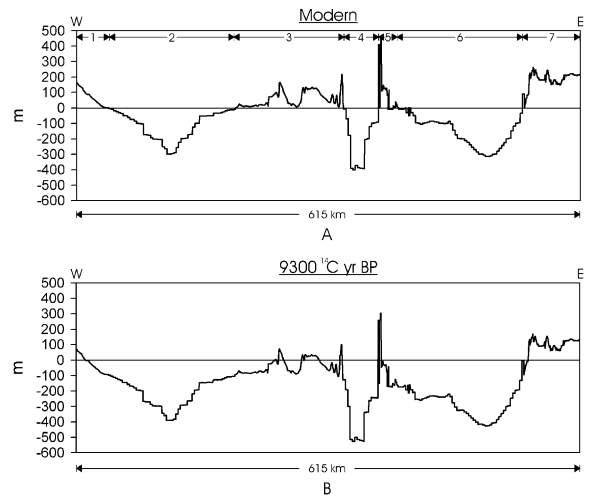


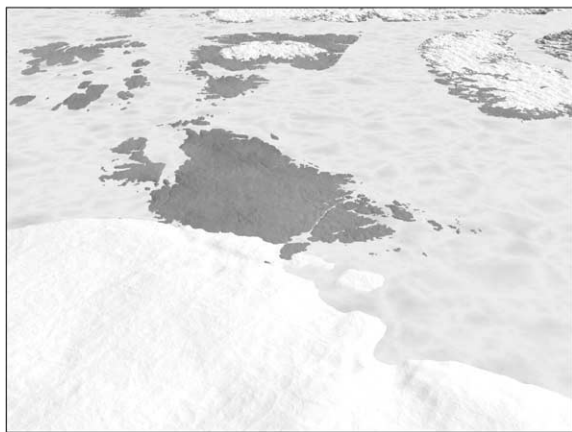
Fig. 7. Topographic cross-sections across 72°N, between 106°W and 88°W, for (A) present day and (B) 9300  $^{14}\text{C}$  yr BP (profile location is given by dashed line in Fig. 2). Elevations in A are given with respect to modern sea level; elevations in B are given with respect to sea level at 9300  $^{14}\text{C}$  yr BP. Numbered horizontal ranges in A correspond to: 1) Victoria Island; 2) M'Clintock Channel; 3) Prince of Wales Island; 4) Franklin Strait; 5) Somerset Island; 6) Gulf of Boothia; and 7) Brodeur Peninsula (Fig. 2). Vertical exaggeration is 190  $\times$ .

significant. Fig. 7 shows two topographic cross-sections along 72°N, from 106°W to 88°W: the first corresponds to modern times and the second corresponds to 9300  $^{14}\text{C}$  yr BP. Along this transect, isobase values for 9300  $^{14}\text{C}$  yr BP range between 87 and 165 m (Fig. 4). The modern cross-section shows three discrete water routes (from west to east: M'Clintock Channel, Franklin Strait, and Gulf of Boothia; Figs. 2 and 7), all of which were considerably larger at 9300  $^{14}\text{C}$  yr BP; the 100 km<sup>2</sup> cross-sectional area of the channels at this time was double the 51 km<sup>2</sup> total cross-sectional area of the three modern channels. Such significant changes in channel cross-sectional area and morphology, which occurred over vast areas of the Canadian Arctic Archipelago during and following deglaciation, must have greatly influenced regional water circulation.

Three-dimensional visualizations generated from the topographic databases of Figs. 3 and 5 are given in Fig. 8. Shown are views of both modern and paleotopography of the central portion of the Canadian Arctic Archipelago. The two visualizations were generated using an identical viewing position situated 125 km above the Canadian arctic mainland, and provide northward views along Boothia Peninsula toward Prince of Wales and Somerset islands, and Brodeur Peninsula (Baffin Island). These visualizations depict the dramatic landscape differences for this region between modern times and 9300  $^{14}\text{C}$  yr BP. These types of visualizations



(A)



(B)

Fig. 8. Three-dimensional visualizations of (A) modern and (B) paleo- (9300  $^{14}\text{Cyr BP}$ ) topography of central portion of Canadian Arctic Archipelago. Visualizations are based on topographic models given in Figs. 3 and 5, and were generated without vertical exaggeration. Each visualization is made from identical viewing position located 125 km above Canadian arctic mainland, and provides northward view along Boothia Peninsula toward Prince of Wales and Somerset islands, and Brodeur Peninsula (Baffin Island) (Fig. 2). Southern extremes of Bathurst, Cornwallis, and Devon islands are visible in farthest distances. For clarity, land surfaces are depicted without snow or ice cover, except where ice caps were present (Somerset, Cornwallis, Devon and Baffin islands) and where Laurentide Ice Sheet covered portions of southern Boothia Peninsula (Fig. 2). Channel surfaces in both visualizations are depicted as completely frozen, which in modern times is typical for most channels in region in winter season (Maxwell, 1982).

can be useful for the communication of information about past Quaternary environments, and can conceivably be used to inspire new scientific ideas and understanding.

## 5. Conclusions

High-resolution digital reconstructions of late Quaternary landscapes can be made using a GIS method that subtracts interpolated isobase values from modern elevations. The principal utility of the GIS method for reconstructing such landscapes is in the relative ease and rapidity with which high-resolution, quantitative, and georeferenced databases of paleo-topography can be generated. The method can also be used for the projection of future topographic configurations in areas of continuing isostatic rebound or depression.

Databases of paleo-topography generated by GIS modelling can be used for a variety of purposes, including: 1) the generation of paleo-topographic maps or three-dimensional models and animations; 2) the estimation of the areas, volumes, aspects, and slopes of individual landforms; and 3) the approximation of paleo-shoreline positions. GIS-based estimates of the dimensions and form of water bodies and landforms can be used to constrain hydrological and climatic models.

## Acknowledgements

The authors would like to thank John Shaw and an anonymous reviewer for their helpful comments on this paper.

## References

- Andrews, J.T., 1966. Pattern of coastal uplift and deglaciation, west Baffin Island, N.W.T. *Geographical Bulletin* 8, 174–193.
- Andrews, J.T., 1970. *A Geomorphological Study of Post-Glacial Uplift with Particular Reference to Arctic Canada*. Institute of British Geographers, Special Publication 2, London, 156pp.
- Andrews, J.T., 1989. Postglacial emergence and submergence. In: Fulton, R.J. (Ed.), *Quaternary Geology of Canada and Greenland*. Geological Survey of Canada, *Geology of Canada*, no. 1, Chapter 8, pp. 546–562.
- Andrews, J.T., McGhee, R., McKenzie-Pollack, L., 1971. Comparison of elevations of archaeological sites and calculated sea levels in Arctic Canada. *Arctic* 24, 210–228.
- Blake Jr., W., 1970. *Studies of glacial history in Arctic Canada*. I. Pumice, radiocarbon dates, and differential postglacial uplift in the eastern Queen Elizabeth Islands. *Canadian Journal of Earth Sciences* 7, 634–664.
- Bryson, R.A., Wendland, W.M., Ives, J.D., Andrews, J.T., 1969. Radiocarbon isochrones on the disintegration of the Laurentide Ice Sheet. *Arctic and Alpine Research* 1, 1–14.
- Burrough, P.A., McDonnell, R.A., 1998. *Principles of Geographical Information Systems*. Oxford University Press, Oxford, 333pp.

- Clark, J.A., 1976. Greenland's rapid postglacial emergence: a result of ice-water gravitational attraction. *Geology* 4, 310–312.
- Clark, J.A., Farrell, W.E., Peltier, W.R., 1978. Global changes in postglacial sea level: a numerical calculation. *Quaternary Research* 9, 265–287.
- Dyke, A.S., 1974. Deglacial chronology and uplift history: northeastern sector, Laurentide Ice Sheet. Institute of Arctic and Alpine Research, Occasional Paper 12, 73pp.
- Dyke, A.S., 1984. Quaternary Geology of Boothia Peninsula and Northern District of Keewatin, Central Canadian Arctic. Geological Survey of Canada, Memoir 407, 26pp.
- Dyke, A.S., 1987. A reinterpretation of glacial and marine limits around the northwestern Laurentide Ice Sheet. *Canadian Journal of Earth Sciences* 24, 591–601.
- Dyke, A.S., 1999. Last glacial maximum and deglaciation of Devon Island, arctic Canada: Support for an innuitian ice sheet. *Quaternary Science Reviews* 18, 393–420.
- Dyke, A.S., Dale, J.E., McNeely, R.N., 1996b. Marine molluscs as indicators of environmental change in glaciated North America and Greenland during the last 18,000 years. *Géographie physique et Quaternaire* 50, 125–184.
- Dyke, A.S., Dredge, L.A., Vincent, J., 1982. Configuration and dynamics of the Laurentide Ice Sheet during the Late Wisconsinan maximum. *Geographie physique et Quaternaire* 36, 5–14.
- Dyke, A.S., England, J., Reimnitz, E., Jetté, H., 1997. Changes in driftwood delivery to the Canadian Arctic Archipelago: the hypothesis of postglacial oscillations of the transpolar drift. *Arctic* 50, 1–16.
- Dyke, A.S., Hooper, J., Savelle, J.M., 1996a. A history of sea ice in the Canadian Arctic Archipelago based on postglacial remains of the bowhead whale (*Balaena mysticetus*). *Arctic* 49, 235–255.
- Dyke, A.S., Morris, T.F., Green, D.E.C., 1991. Postglacial Tectonic and Sea Level History of the Central Canadian Arctic. Geological Survey of Canada, Bulletin 397, 56pp.
- Dyke, A.S., Prest, V.K., 1987. Paleogeography of Northern North America, 18 000–5000 Years Ago. Geological Survey of Canada, Map 1703A, scale 1:12 500 000.
- EDC DAAC, 1996. GTOPO 30 Database. EROS Data Center Distributed Active Archive Center, US Geological Survey, EROS Data Center, Sioux Falls, South Dakota.
- England, J., 1998. Support for the Innuitian Ice Sheet in the Canadian High Arctic during the last glacial maximum. *Journal of Quaternary Science* 13, 275–280.
- England, J., 1999. Coalescent Greenland and Innuitian ice during the last glacial maximum: revising the Quaternary of the Canadian High Arctic. *Quaternary Science Reviews* 18, 421–456.
- Farrell, W.E., Clark, J.A., 1976. On postglacial sea level. *Geophysics Journal of the Royal Astronomical Society* 46, 647–667.
- Gareau, P., Lewis, C.F.M., Sherin, A., Macnab, R., 1998. The paleo-Great Lakes, their areas and volumes from digital elevation model studies. In: Geological Society of America Annual Meeting, Abstracts with Programs, Toronto, Ontario, p. A-163.
- GLOBE Task Team, 1999. The Global One-kilometer Base Elevation (GLOBE) Elevation Model, Version 1.0. Hastings, D.A., Dunbar, P.K., Elphinstone, G.M., Bootz, M., Murakami, H., Maruyami, H., Masaharu, H., Holland, P., Payne, J., Bryant, N., Logan, T.L., Muller, J.-P., Schreier, G., MacDonald, J.S., (Eds.), National Oceanic and Atmospheric Administration, National Geophysical Data Center, Boulder, Colorado.
- Hastings, D.A., Dunbar, P.K., 1998. Development and assessment of the Global Land One-km Base Elevation Digital Elevation Model (GLOBE). *ISPRS Archives* 32 (4), 218–221.
- Hodgson, D.A., Vincent, J.-S., Fyles, J.G., 1984. Quaternary Geology of Central Melville Island, Northwest Territories. Geological Survey of Canada, Paper 83-16. 25pp.
- Johnston, W.A., 1946. Glacial Lake Agassiz with special reference to the mode of deformation of the beaches. Geological Survey of Canada, Bulletin 7, 20pp.
- JPL, 1998. Shuttle Radar Topography Mission, National Aeronautics and Space Administration, Jet Propulsion Laboratory, Technical Factsheet JPL 400-713, 2pp.
- Lambeck, K., 1996. Shoreline reconstructions for the Persian Gulf since the last glacial maximum. *Earth and Planetary Science Letters* 142, 43–57.
- Leverington, D.W., Mann, J.D., Teller, J.T., 2000. Changes in the bathymetry and volume of glacial Lake Agassiz between 11,000 and 9300 <sup>14</sup>Cyr BP. *Quaternary Research* 54, 174–181.
- Lewis, C.F.M., Gareau, P., 2001. Evaluating glacio-isostatic uplift from tilted shoreline data to reconstruct the paleobathymetry and topography of the Great Lakes basin. In: 27th Annual Scientific Meeting of the Canadian Geophysical Union, Program and Abstracts, Ottawa, Ontario.
- Mann, J.D., Leverington, D.W., Rayburn, J.A., Grant, N., Teller, J.T., 1997. Calculating the volume and heat budget of glacial Lake Agassiz. In: Geological Society of America Annual Meeting, Abstracts with Programs, Salt Lake City, Utah, p. A-111.
- Mann, J.D., Leverington, D.W., Rayburn, J., Teller, J.T., 1999. The volume and paleobathymetry of glacial Lake Agassiz. *Journal of Paleolimnology* 22, 71–80.
- Maxwell, J.B., 1982. The Climate of the Canadian Arctic Islands and Adjacent Waters, Vol. 2, Climatological Studies 30, Atmospheric Environment Service, Toronto, 589pp.
- Mayewski, P.A., Denson, G.H., Hughes, T.J., 1981. Late Wisconsin ice sheets in North America. In: Denton, G.H., Hughes, T.J. (Eds.), *The Last Great Ice Sheets*. Wiley, New York, pp. 67–178.
- McCann, S.B., Chorley, R.J., 1967. Trend surface mapping of raised shorelines. *Nature* 215, 611–612.
- NGDC, 1988. ETOPO 5 Database, Data Announcement 88-MGG-02. In: *Digital Relief of the Surface of the Earth*. NOAA, National Geophysical Data Center, Boulder, Colorado.
- Peltier, W.R., 1974. The impulse response of a Maxwell Earth. *Reviews of Geophysics and Space Physics* 12, 649–669.
- Peltier, W.R., 1985. The LAGEOS constraint on deep mantle viscosity; results from a new normal mode method for the inversion of viscoelastic relaxation spectra. *Journal of Geophysical Research* 90, 9411–9421.
- Peltier, W.R., Andrews, J.T., 1976. Glacial-isostatic adjustment – I. The forward problem. *Geophysical Journal of the Royal Astronomical Society* 46, 605–646.

- Peucker, T.K., Fowler, R.J., Little, J.J., Mark, D.M., 1978. The triangulated irregular network. In: Proceedings of the DTM Symposium. American Society of Photogrammetry - American Congress on Survey and Mapping, St. Louis, Missouri, pp. 24–31.
- Smith, D.E., Sissons, J.B., Cullingford, R.A., 1969. Isobases for the Main Perth raised shoreline in south-east Scotland as determined by trend-surface analysis. *Transactions of the Institute of British Geographers* 46, 45–52.
- Walcott, R.I., 1970. Isostatic response to loading of the crust in Canada. *Canadian Journal of Earth Sciences* 7, 716–727.
- Walcott, R.I., 1972. Late Quaternary vertical movements in eastern North America: quantitative evidence of glacio-isostatic rebound. *Reviews of Geophysics and Space Physics* 10, 849–884.
- Wolfe, A.P., King, R.H., 1999. A paleolimnological constraint to the extent of the last glaciation on northern Devon Island, Canadian High Arctic. *Quaternary Science Reviews* 18, 1563–1568.